CONF-9005107--1

SAND--90-0077C

DE90 006535

THE VISCOELASTICITY OF CURING THERMOSETS

Douglas Adolf and James E. Martin
Sandia National Laboratories
Albuquerque, NM 87185

Abstract

As a crosslinking polymer cures, dramatic changes in molecular architecture occur. These structural changes in turn affect the viscoelastic behavior of the material. At a critical extent of reaction (the gel point), the polymer undergoes a transition from a viscous liquid to an elastic solid. We have monitored the evolution of structure and viscoelasticity in an epoxy encapsulant used at Sandia, the diglycidyl ether of Bisphenol A (BADGE) cured with diethanolamine (DEA). The structure evolves according to percolation theory, and the viscoelasticity evolves according to our dynamic scaling theory for branched polymers.

Introduction

Crosslinked epoxies are used extensively at Sandia as encapsulating compounds for electronic components. The rigid polymer physically holds component boards in place and provides increased dielectric strength. The purpose of this paper is to document the changes in the structure and viscoelastic response of a common encapsulating epoxy, the diglycidyl ether of Bisphenol A (BADGE) cured with diethanolamine (DEA).

Evolution of Structure

The simplest theories for describing how the average molecular weight and size of the clusters increases as the reaction progresses are the mean-field theories of Flory and Stockmayer [1]. These assume that each functional group is equally reactive and that no intra-cluster cyclization occurs. Therefore, at the beginning of the reaction, when there is mainly monomer, the molecular weight of a single cluster will increase by one monomer each time a reaction takes place. As the reaction progresses and many large clusters form, each reaction will join clusters. At some point, if each monomer has a functionality of f>2, we reach a critical extent of reaction, α_c, at which the average molecular weight approaches infinity. Beyond the gel point, finite clusters continue to attach to the infinte cluster (i.e. the gel) increasing the gel fraction and the equilibrium modulus.

In the rest of this report, we will not refer directly to the extent of reaction, α, but to the reduced extent of reaction relative to the gel point, $\varepsilon = |p_c - p|/p_c$ where p is the crosslink probability and p_c is that at the gel point. To determine p, we must remember that our system does not consist simply of the crosslinker DEA as assumed in the previous paragraph, but also includes the difunctional epoxy. Therefore, the crosslink probability, p, is not just the epoxy reaction probability, α. Instead both epoxy groups on the BADGE must react to form a crosslink, and $p = \alpha^2$ giving $\varepsilon = |\alpha_c^2 - \alpha^2|/\alpha_c^2$.

The simple mean-field arguments above can be solved analytically and predict that, near the gel point, the sol weight-average molecular weight as determined by light scattering should diverge as ε^{-1}. The distribution of molecular weights in this "critical regime" is predicted to follow the power law, $n(M) \sim M^{-5/2}$, up to the z-average molecular weight above which it decays exponentially. The z-average cluster size as measured by light scattering is predicted to diverge as $\varepsilon^{-1/2}$.

Recently, another theory for gelation has been developed called percolation [2]. While not amenable to analytic treatment, percolation does offer simple physical insight into gelation. We first establish a lattice of arbitrary structure (e.g. cubic or hexagonal in three dimensions). Upon each node of the lattice, we place a monomer with the functionality of the lattice (e.g. functionality 6 for a cubic lattice). Now, at random, we connect adjacent monomers forming a bond or crosslink. Note that intra-cyclization is now allowed. The bond probability, p, is simply the number of bonds formed at a given time divided by the total number of bonds possible.

Computer simulations of percolation have shown that it too exhibits power law divergences of the weight-average molecular weight and z-average cluster size when sufficiently close to the gel point but with different exponents than the mean-field theories. Specifically, $M_w \sim \varepsilon^{-16/9}$ and $R_z \sim \varepsilon^{-8/9}$. The distribution of molecular weights is described by $n(M) \sim M^{-11/5}$ up to M_z with an exponential decay. Percolating structures also exhibit the powerful feature of self-similarity, which implies that pictures of the sol taken at the gel point are identical regardless of magnification. This is equivalent to stating that the system at the gel point has no characteristic length scale. Self-similarity will become extremely important when describing the dynamics of crosslinking systems.

There also exists self-similarity within a single cluster as shown by the "fractal" nature of computer generated percolation clusters. That is, if we look within a cluster with a window of size r, we cannot gauge the size of the window by our view; again, there is no characteristic length. This in turn implies that the mass distribution within the window behaves as $m \sim r^D$ where D is called the fractal dimension of the cluster. This relationship will also apply for the overall mass and size of a single cluster so that $M \sim R^D$. Obviously, D must be greater than 1 (a rod) and less than 3 (a sphere) in 3-dimensional space. Percolation predicts that D = 5/2 whereas mean-field theories predict that D = 4. This is the first clue that mean-field theories are not correct. They generate clusters that cannot physically fit in 3-d space!

The percolation predictions for the critical exponents are independent of the type of lattice used. For example, $M_w \sim \varepsilon^{-16/9}$ for a cubic or hexagonal 3-d lattice and only the bond probability at the gel point changes. This implies that an exact description of the chemical kinetics is unnecessary since it should not affect the critical exponents, but only change the fraction of epoxy groups reacted at the gel point. However, the *dimensionality* of the lattice does change the numerical values for the exponents. In fact, mean-field theories have been found to be a special case of percolation for the spatial dimension equal to 6 (a rather unpleasant dimension in which to live). In 6 dimensions, there is enough room so that the mean-field assumption of no intra-cluster circuits becomes reasonable. This is another clue that the mean-field theory may not accurately describe gelation.

Of course, percolation may not accurately describe gelation either. For example, percolation ignores all dynamics of the clusters which may be important. By measuring the critical exponents describing the divergence of M_w and R_z near the gel point by light scattering, we can determine if either mean-field theories or percolation are models for the crosslinking of our BADGE/DEA epoxy. As shown in the following table, the predictions are so different that it should be easy to distinguish between the two.

critical exponent	percolation prediction	mean-field prediction
$M_w \sim \varepsilon^{-\gamma}$	$\gamma = 16/9$	$\gamma = 1$
$R_z \sim \varepsilon^{-\nu}$	$\nu = 8/9$	$\nu = 1/2$

The divergences of the molecular weight and radius were measured [3] by quenching aliquots taken from the reaction bath at known intervals up to the gel point by dilution in a 60/40 toluene/isopropanol solution. The gel time, t_c (approximately 3 hours), was taken to be the midpoint between the time at which the first insoluble aliquot was taken and the time at which the last soluble aliquot was taken. From this, we calculated ε using FTIR measurements of extent of reaction versus time. The extent of reaction at the gel point corresponds to approximately 65% of the epoxy groups reacted that are present after the initial DEA amine endcapping. The weight average molecular weights were then measured with a low angle light scattering photometer (at

concentrations of 10 to 50 mg/ml and solid angles of 4-5 and 6-7°). The z-average hydrodynamic radii were measured using a HeNe laser operating at 633 nm at a scattering angle of 20°. A cumulant analysis obtained from a 256 channel Langley-Ford digital correlator was used to obtain the relaxation time, and the hydrodynamic radii were obtained using Stokes law and the known solvent viscosity.

In Figure 1, we show the divergences of the weight-average molecular weight and the z-average hydrodynamic radius as the gel point is approached. The slopes are 1.7 ± 0.1 and 1.4 ± 0.1 respectively. While the slope 1.7 ± 0.1 gives the critical exponent, γ, the slope 1.4 ± 0.1 is not directly equal to ν since the sol clusters swell as they are transferred from the reaction bath to the solvent. To relate the divergence of the swollen hydrodynamic radius to the unswollen divergence, we have used standard literature arguments that balance the osmotic swelling force against the elastic restoring force. These arguments reduce the slope 1.4 ± 0.1 by a factor of 0.8 such that $\nu = 1.1 \pm 0.1$. The experimental results $\gamma = 1.7 \pm 0.1$ and $\nu = 1.1 \pm 0.1$ should be compared to the mean field an percolation predictions in the table on the previous page. We see that the measured values are in good agreement with the percolation predictions. The measured ν is slightly larger than predicted; however, it cannot be determined from these experiments whether this is due to the actual divergence of the average size or to the arguments used to account for swelling upon dilution.

Since percolation seems to describe the evolution of structure in our epoxy encapsulant, we can now use the concept of self-similarity to help derive a theory for the evolution of viscoelasticity during crosslinking.

Viscoelasticity: Theoretical Foundation

As we have seen above, a crosslinking system undergoes a liquid-to-solid transition at the gel point. However, the dynamic response of the system to an imposed deformation is more complicated than simply purely viscous or elastic. For example, the branched sol molecules formed during cure have a spectrum of relaxation times and, therefore, are purely elastic at short times ($t<\tau_1$ where τ_1 is the shortest relaxation time) and purely viscous at very long times ($t>\tau_N$ where τ_N is the longest relaxation time). The intermediate viscoelastic response is closely related to the structure of the molecules, so our previous studies on the evolution of structure will guide us.

Before discussing branched polymers, it is useful to present theories for the apparently simpler *linear* polymers [4]. If the chains in the melt are relatively short, the dynamical response of a single chain can be modelled as a string of N Brownian beads connected by N-1 Hookean springs. Therefore, the stress relaxation modulus G(t), which is the ratio of the resultant stress $\sigma(t)$ to a suddenly applied strain γ, is just a sum of the individual relaxation modes $G(t) \sim \Sigma \exp(-t/\tau_k)$ where τ_k are the relaxation times for the polymer. The longest relaxation time, τ_N, is dependent on the molecular weight of the chain. We can determine this molecular weight dependence as follows. Since a chain diffuses a distance proportional to its radius R in a time τ_N, $\tau_N \sim R^2/D_t$ where D_t is the translational diffusion coefficient of the polymer. A linear chain in a melt traces a random walk configuration so $R \sim N^{1/2}$ (i.e. linear chains have a fractal dimension of 2). In the simplest version, D_t is simply proportional to $(N\zeta)^{-1}$ where ζ is the friction of one bead; that is, each bead contributes ζ to the chain friction. Therefore, $\tau_N \sim R^2/D_t \sim N/(N^{-1}) \sim N^2$.

If we calculate the spectrum of relaxation times for this simple model, we find that $\tau_k \sim (k/N)^{\alpha} \tau_N$. The exponent α is found by noting that the first relaxation time, τ_1, is due to coordinated

motion of several atoms and, therefore, must be independent of the molecular weight (N) of the chain so $\tau_1 \sim N^{-\alpha}\ \tau_N \sim N^{-\alpha}\ N^2 \sim N^0$. We find, then, that $\alpha = 2$. The scaling behavior of the relaxation times reflects the self-similar nature of the linear polymer chains. Again, if we look at an ideal polymer chain with a window of size r<R, we cannot gauge the size of the window by our view. The fractal *structure* of the polymer simplifies the *dynamics*. We will use these concepts in our discussion of the dynamics of branched polymers as well.

Our first attempt at describing the dynamics of crosslinking polymers, then, will start from the same point: a bead-spring model for branched polymers [5,6]. The theory is analogous to that for linear chains. The stress relaxation modulus, G(t), for a single chain again will be the sum over normal modes. Since the percolation clusters formed during crosslinking are fractal objects, we will again assume that the relaxation times scale as the longest relaxation time for that cluster $\tau_k \sim (k/N)^{\alpha}\ \tau_N$ where $\tau_N \sim R^2/D_t$. However, the fractal dimension of the percolation clusters is now 5/2 instead of 2 as for linear chains. This leads to $\alpha = 9/5$ so $\tau_N \sim N^{9/5}$.

Now we must account for the broad polydispersity exhibited by percolating systems. As we saw above, percolation predicts that the cluster distribution is given by $n(M) \sim M^{-11/5} \exp(-M/M_z)$ where M_z is the z-average molecular weight. To calculate the stress relaxation modulus for the entire reaction bath, we simply sum the result above for a single cluster over all clusters

$$G(t) \sim \int_1^M dM\, n(M) \sum_{k=1}^{M} e^{-t/\tau_k} \qquad (1)$$

This integral cannot be solved analytically, but does yield closed form results in certain limits. For example, for $\tau_1 << t << \tau_z$, $G(t) \sim t^{-\Delta} \sim t^{-2/3}$. The time τ_z is the longest relaxation time for the cluster of mass M_z (which defines the cutoff in the power law polydispersity) and scales as $\tau_z \sim R_z^2/D_t(R_z) \sim R_z^{9/2}$. Using the percolation prediction for the divergence of the z-averaged radius (which we saw agreed well with our experimental value), $\tau_z \sim \varepsilon^{-4}$ where $\varepsilon = |\alpha_c^2 - \alpha^2|/\alpha_c^2$ as before. Therefore, τ_z diverges as we approach the gel point. The power law relationship for G(t) reflects that the system has no characteristic time for $\tau_1 < t < \tau_z$ which itself arises from the lack of a characteristic length for $a < r < R_z$ (where a is the monomer size). For $t >> \tau_z$, we can also solve the integral above and obtain $G(t) \sim \exp(-t/\tau_z)^b$ where b=2/5. A useful form for fitting data over all time is

$$G(t) = A\,\frac{\eta}{\tau_z}\left(\frac{\tau_z}{t}\right)^{\Delta} e^{-(t/\tau_z)^b} \qquad (2)$$

where b=0.4 and A is just a numerical prefactor dependent on the particular system chosen.

From the theory of linear viscoelasticity, the steady-state zero-shear rate viscosity is the integral of the stress relaxation modulus over all time. This integration yields $\eta \sim M_w^{3/4} \sim \varepsilon^{-4/3}$ which describes how fast the viscosity diverges as we approach the gel point. Linear viscoelastic theory also states that the stored elastic energy in the sol is quantified by the reciprocal of the steady-state creep compliance, $J_e^o = \tau_z/\eta \sim \varepsilon^{-8/3}$.

We cannot directly calculate the equilibrium modulus, G_∞, beyond the gel point. However, we can make one of two physically reasonable assumptions: (1) G_∞, which defines the elastically stored energy in the gel, scales as its counterpart $(J_e^o)^{-1}$ for the sol or (2) the longest relaxation time for the gel scales as its counterpart, τ_z, for the sol. Either of these assumptions yield $G_\infty \sim \varepsilon^{8/3}$. Using Eq. 2 and the scaling relationship $G_\infty \sim \eta/\tau_z$, we can now write an expression for the stress relaxation modulus for the gel

$$G(t) = G_\infty \left[1 + B\left(\frac{\tau_z}{t}\right)^{\Delta} e^{-(t/\tau_z)^b} \right] \qquad (3)$$

where B is another constant dependent on the chemistry of the chosen system.

Thus Eqs. 2 and 3 describe master curves when the absicca and ordinate are scaled by τ_z and G_∞ (i.e. ε^z) respectively. This constitutes a viscoelastic superposition principle, *time-cure superposition* [7], and is, of course, valid for any viscoelastic function. For example, the complex shear modulus that describes the response of the system to a sinusiodal oscillation can be expressed as the universal function $G^*(\omega\tau_z)/G_\infty$.

It is important to emphasize that the theory presented above is dependent on the self-similarity concepts of percolation. Remember that percolation only predicts self-similarity and power-law behavior when sufficiently "close" to the gel point. Therefore, our theory, which predicts critical exponents, will be valid only over some range or extents of reaction that must be determined experimentally. It is not possible to tell beforehand how large this critical regime will be.

Viscoelasticity: Experimental Studies

We first tested our theory by directly measuring the divergence of the bulk viscosity [3] at 90°C using a Rheometrics RDS-2 with 50mm diameter parallel plates close to the gel point and a Brookfield viscometer LVTDV-II with spindle 1 in a 10-cm diameter beaker at 0.3 to 30 RPM farther away from the gel point. The instrumental torques were monitored continuously up to full scale at constant shear rate at 90°C . By taking several runs at different shear rates, we determined that the measured viscosity was Newtonian up to roughly 10,000 Poise at a shear rate of $4x10^{-3}$ rad/sec. Determination of the gel time is difficult in this experiment. We followed the standard procedure of plotting log η against log ε for various values of the gel time and used that value which resulted in the most linear relationship. In Figure 2, the measured slope is 1.4 ± 0.2 which is excellent agreement with the theoretical prediction of 4/3. We also see that one exponent can describe the divergence of the viscosity for $\varepsilon < 0.52$, or in terms of the extent of reaction, $0.45<\alpha<\alpha_c$ (=0.65). Therefore, the "critical regime" where our scaling theory should apply is given by these bounds.

We next attempted to verify the time-cure superposition principle [8] suggested by Eq.s 2 and 3. It is difficult to measure directly the time-dependent shear relaxation modulus, so we measured instead the in-phase (G'=storage modulus) and out-of-phase (G"=loss modulus) components of the complex shear modulus, G*, described above. The measurements were performed on the Rheometrics RDS-2 between 50mm parallel plates at 0.2 to 2% strain that were kept at 90°C. Frequency scans from 2 to 200 radians/second were taken approximately every 4 minutes with each scan lasting just over a minute. The gel time of 188 minutes was not left as an adjustable parameter but was independently determined as the time at which $G'(\omega) \sim G"(\omega) \sim \omega^{\Delta}$ strictly applied.

Figures 3 and 4 show the master curves that result from time-cure superposition. Here the frequency and the modulus (G*) for each value of ε were shifted by factors proportional to ε^{-y} and ε^z respectively. The parameters z and y were chosen to be those giving the best superposition for G' and G" both before and after the gel point. Therefore, there are four independent sets of data from which we have extracted the exponents z and y. Excellent superposition is achieved with z=2.8 (±0.2) and y=3.9 (±0.2), and these agree very well with the predictions z=8/3 and y=4 of the dynamic scaling theory.

We have also measured the increase in the equilibrium modulus with extent of reaction

directly. The samples were cured at 90°C in rectangular geometry (2.5" x 0.5" x 0.25") to differing extents past the gel point and placed in the RDS-2. The storage modulus G' was measured at 90°C as a function of time at a fixed frequency of 1 radian/second. In Figure 2, we have plotted the increase of the equilibrium modulus as determined by time-cure superposition and by these direct measurement on partially cured BADGE/DEA samples. The measurements agree well with each other and are within experimental error of the theoretical predictions (z=8.3). The breadth of the critical regime where the theory applies is surprising. Within error, the divergence of the equilibrium modulus is described by a single exponent over the *entire* post gel regime. This broad critical regime is no doubt due in part to the extremely low molecular weight of the epoxy chains (MW=380), but that it extends over the entire post-gel region is very surprising.

Conclusions

We have seen that percolation accurately reflects the evolution of structure in our most common epoxy encapsulant, DEA-cured BADGE. We can benefit from this agreement by using the self-similarity concepts from percolation to help develop a scaling theory for the viscoelasticity for crosslinking systems. The critical divergences predicted by such a theory are in excellent agreement with those measured in our 828/DEA epoxy. In addition, the theory suggests that data taken at various extents of reaction should have identical functional forms and simply rescaling the ordinate and abscissa by the appropriate factors should produce master curves. Such superposition is observed in the BADGE/DEA system, and the shift factors agree well with the theoretical predictions.

While we studied a system of interest to Sandia, we should stress that the dynamic scaling theory should apply equally well to any crosslinking system *in the critical regime*. The question remains "How large is the critical regime?" We showed that the critical regime extends over half of the reaction for the BADGE/DEA system due to the small size of the reacting monomers. For other small monomer systems, the theory should be equally valid and the critical regime should extend over a comparable range.

References

(1) Flory, P. J. *Principles of Polymer Chemistry*; Cornell University Press: Ithaca, NY, 1953.

(2) Stauffer, D. *Introduction to Percolation Theory*, Taylor and Francis: London, 1985.

(3) Adolf, D.; Martin, J. E.; Wilcoxon, J. P. "Evolution of Structure and Viscoelasticiy in an Epoxy Near the Sol-Gel Transition" submitted to *Macromolecules.*

(4) Ferry, J. D. *Viscoelastic Properties of Polymers*; Wiley: New York, 1980.

(5) Martin, J. E.; Adolf, D.; Wilcoxon, J. P. "Viscoelasticity of Near-Critical Gels" *Phys. Rev. Lett.* **1988**, *61*, 2620.

(6) Martin, J. E.; Adolf, D.; Wilcoxon, J. P. "Viscoelasticity Near the Sol-Gel Transition" *Phys. Rev. A* **1989**, *39*, 1325.

(7) Adolf, D.; Martin, J. E. "Time-Cure Superposition Curing Crosslinking" submitted to *Macromolecules.*

Figure Captions

FIG. 1: Divergence of the weight-average molecular weight and z-average radius for the sol.

FIG. 2: Divergence of the viscosity for the sol and the equilibrium modulus for the gel.

FIG. 3: Time-cure superposition of the storage and loss moduli for the sol.

FIG. 4: Time-cure superposition of the storage and loss moduli for the gel.

Figure 1

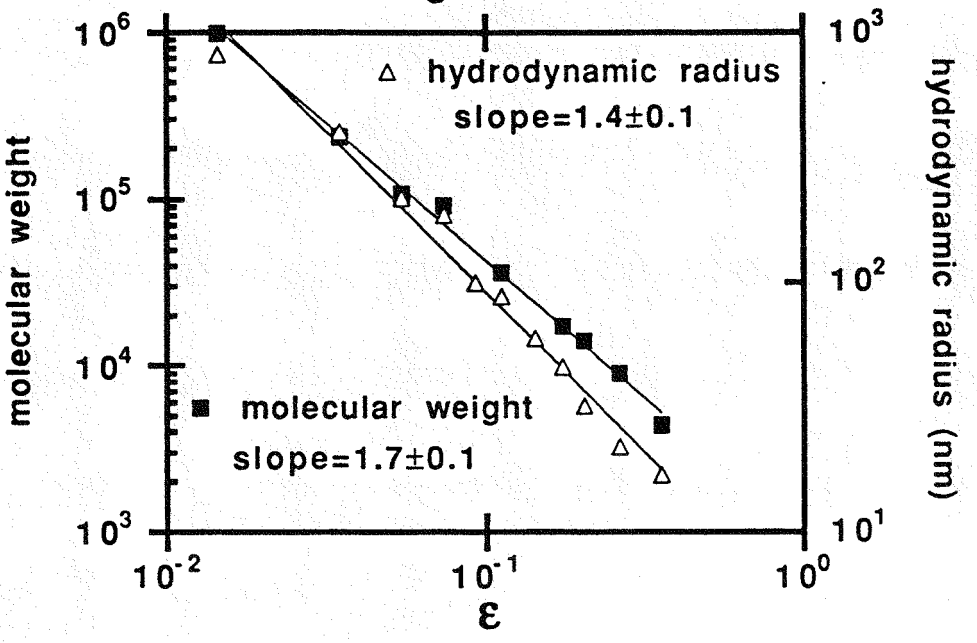

Figure 2

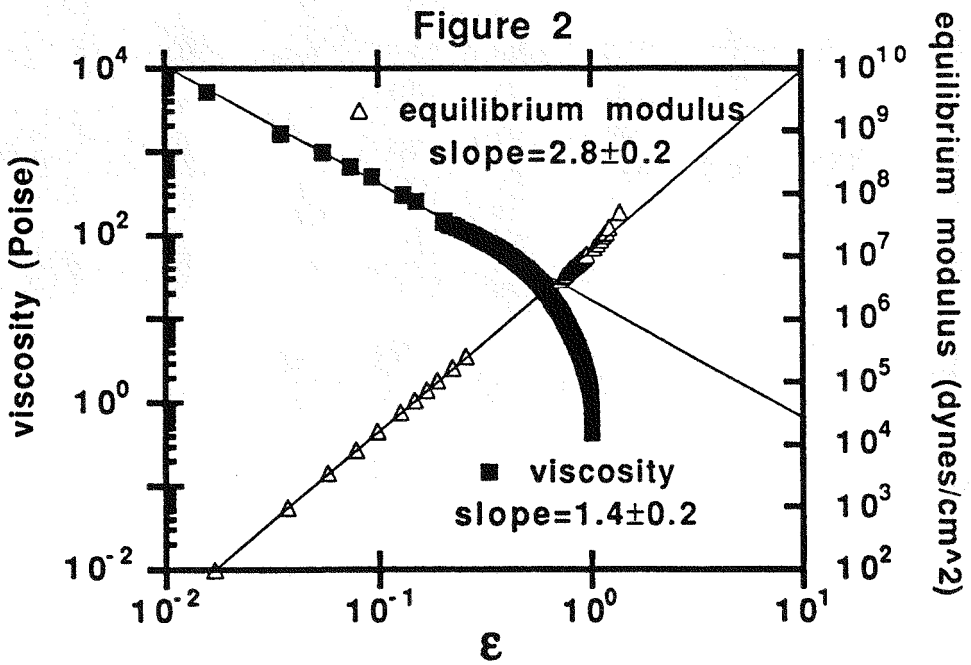

Figure 3

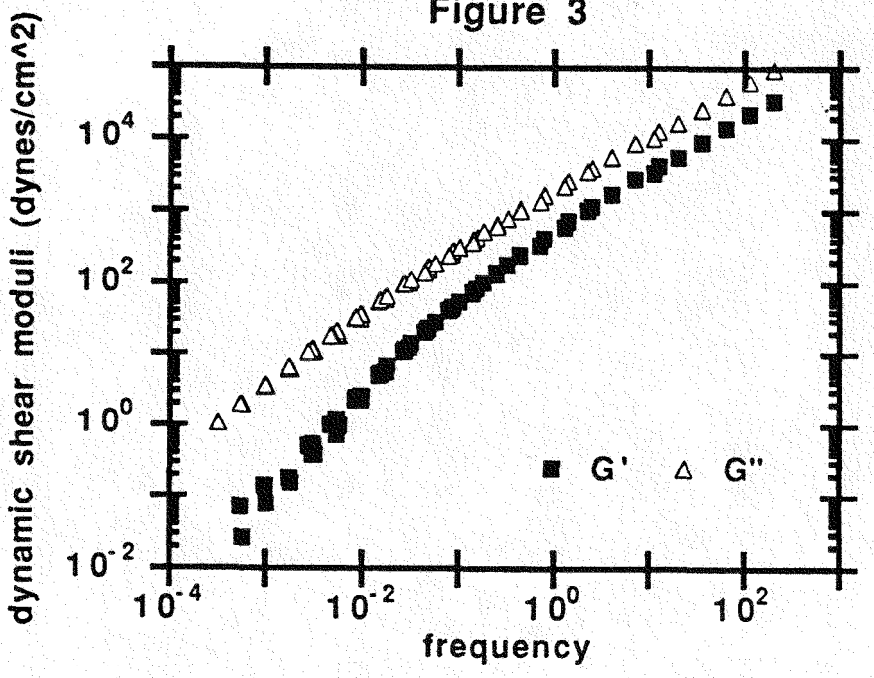

Figure 4